On the prediction of hot spot induced ignition by the Livengood-Wu integral

Xinyi Chen[1], Peng Zhao[2], Peng Dai[3], Zheng Chen[1]

[1] SKLTCS, CAPT, BIC-ESAT, Department of Mechanics and Engineering Science, College of Engineering, Peking University, Beijing 100871, China

[2] Department of Mechanical Engineering, Oakland University, Rochester, MI 48309, USA

[3] Department of Mechanics and Aerospace Engineering, Southern University of Science and Technology, Shenzhen 518055, China

Corresponding author: Zheng Chen, Ph.D.

State Key Laboratory for Turbulence and Complex Systems
Department of Mechanics and Engineering Science,
College of Engineering, Peking University
Beijing 100871, China
Tel: +86-(10) 6276-6232
Email: cz@pku.edu.cn

Colloquium topic: Fire Research

Paper length (method 1):

Main Text:	word processor count	= 3370
Equations:	(8 line + 2) × (7.6 words/line) × (1 column)	= 76
References:	(37+2)×(2.3 lines/reference) × (7.6 words/line)	= 682
Figure Captions:	word processor count	= 358
Figure 1:	(73 mm+10) × (2.2 words/mm) × (2 column)	= 182
Figure 2:	(47 mm+10) × (2.2 words/mm) × (2 column)	= 125
Figure 3:	(53 mm+10) × (2.2 words/mm) × (1 column)	= 138
Figure 4:	(53 mm+10) × (2.2 words/mm) × (1 column)	= 138
Figure 5:	(53 mm+10) × (2.2 words/mm) × (1 column)	= 138
Figure 6:	(53 mm+10) × (2.2 words/mm) × (1 column)	= 138
Figure 7:	(53 mm+10) × (2.2 words/mm) × (1 column)	= 138
Figure 8:	(53 mm+10) × (2.2 words/mm) × (2 column)	= 138
Figure 9:	(53 mm+10) × (2.2 words/mm) × (2 column)	= 138
Figure 10:	(53 mm+10) × (2.2 words/mm) × (2 column)	= 138
Figure 11:	(50 mm+10) × (2.2 words/mm) × (2 column)	= 132
Figure 12:	(53 mm+10) × (2.2 words/mm) × (2 column)	= 138
	Total	**= 6170 words**

Supplementary Material: no

Color reproduction: no (all color figures are to be printed in gray scale)

On the prediction of hot spot induced ignition by the Livengood-Wu integral

Xinyi Chen[1], Peng Zhao[2], Peng Dai[3], Zheng Chen[1,*]

[1] SKLTCS, CAPT, BIC-ESAT, Department of Mechanics and Engineering Science, College of Engineering, Peking University, Beijing 100871, China

[2] Department of Mechanical Engineering, Oakland University, Rochester, MI 48309, USA

[3] Department of Mechanics and Aerospace Engineering, Southern University of Science and Technology, Shenzhen 518055, China

Abstract

The Livengood-Wu (L-W) integral is popularly used to predict the occurrence of homogeneous autoignition without heat and mass transport; yet it has not been used for non-homogeneous forced ignition which usually occurs in fire or explosion accidents. In this study, the forced ignition process caused by a hot spot in a flammable mixture is considered, and a method using the L-W integral is developed to predict the critical ignition temperature. In this method, the evolution of the temperature at the hot spot center is first obtained by solving the one-dimensional unsteady heat conduction equation. Then the L-W integral is evaluated based on the central temperature evolution and the corresponding homogenous ignition delay time. The critical ignition temperature is determined at the condition when the L-W integral reaches unity. The present method based on the L-W integral can reduce the computational cost by two to three orders compared to the detailed transient simulation considering detailed chemistry and transport. Different fuels including methane, hydrogen, n-heptane, and dimethyl ether are considered. The predicted critical ignition temperature based on the L-W integral is compared with that predicted by one-dimensional transient simulations considering detailed chemistry and transport. For hydrogen, the present method based on the L-W integral can accurately predict the critical ignition temperature. However, for the other three fuels, the predicted critical temperature is lower than that from detailed simulation. Such under-prediction is interpreted by the ratio between the time scales for ignition and mass diffusion. Nevertheless, the method based on the L-W integral can give a conservative prediction of the critical ignition temperature, which is important for fire safety considerations. Besides, the effects of low temperature chemistry (LTC) on hot spot induced ignition are examined. It is found that the hot spot induced ignition is mainly controlled by high temperature chemistry.

Keywords: Ignition; hot spot; Livengood-Wu integral; critical ignition temperature

* Corresponding author. E-mail: cz@pku.edu.cn, Tel: 86-10-62766232.

1. Introduction

Ignition is a thermal-chemical process where a flammable mixture is brought to a state of rapid combustion [1]. Understanding ignition is important not only for fundamental combustion research but also for fire safety control. Typically, there are two types of ignition: autoignition and forced ignition. Autoignition is closely related to abnormal combustion (e.g., knocking) in internal combustion engines (ICEs) [2]. To predict the occurrence of autoignition in ICEs, Livengood and Wu [3] proposed an integration method describing the process of a mixture advancing towards ignition with the accumulation of chain carriers. In the so-called Livengood-Wu (L-W) integral, the reactivity of a specific mixture is represented by the inverse of ignition delay. Successful autoignition occurs when the value of the L-W integral reaches unity [3]. Recently, the L-W integral has been extended for fuels with two-stage ignition [4, 5], and Zhao and his coworkers [6, 7] have developed the staged L-W integral to evaluate and predict the two-stage autoignition behaviors of different primary reference fuels. Due to its simplicity and low computational cost, the L-W integral has been widely used in the prediction of autoignition in engines and other ignition processes with varying thermodynamic conditions [2, 8-12].

A typical forced ignition scenario is hot spot induced ignition in a flammable mixture, which is a major fire hazard that occurs at many situations, especially in mining, manufacturing, and aviation sectors [13]. A hot spot can be generated by potential ignition sources including hot droplet, hot particle, hot surface, and local spark. When the temperature of the hot spot is above certain critical value, successful ignition can be induced which may cause subsequent flame propagation, deflagration to detonation transition or even catastrophic explosion under certain conditions. Moreover, hot spot induced ignition is closely related to the so-called spot fire which can cause extensive damage to buildings, land and lives [14-16]. Therefore, predicting the critical ignition temperature of hot spot induced ignition is extremely important for fire safety considerations.

Due to the large temperature gradient between the hot spot and the surrounding bulk mixtures, temperature in the hot spot decreases through heat conduction. Following the Semenov criterion [17],

successful hot spot induced ignition occurs only when the chemical heat release rate is higher than the conductive heat loss rate. Therefore, the hot spot induced ignition is controlled not only by chemical reactions but also by heat transfer [1, 18]. Moreover, preferential diffusion and radical loss associated with mass transfer can also change the local equivalence ratio and chemical reactivity in the ignition kernel [19], which further complicates the ignition process triggered by a hot spot. The critical ignition temperature of the hot spot can be predicted through transient simulations considering detailed chemistry and transport. However, such simulation is very time consuming, especially for fuels with large chemistry. Due to its low computational cost and satisfactory predictability, the L-W integral has been widely used for homogenous autoignition, where heat and mass transfer is absent. In the current work, for the first time, it is used to understand and predict forced ignition caused by a hot spot. The objective is to develop a method based on the L-W integral to predict the critical ignition temperature of hot spot induced ignition. The predicted critical ignition temperature for different fuels will be compared with those from one-dimensional transient simulations considering detailed chemistry and transport. The limitation of the present method based on the L-W integral will be discussed. Besides, the effects of low temperature chemistry (LTC) on hot spot induced ignition will be examined for typical conditions concerning fire safety.

2. Model and methods

Here we consider the forced ignition process caused by a hot spot in a static fuel/air mixture with the initial temperature of T_0=300 K. The pressure is fixed to be P=1 atm. Different fuels including methane, hydrogen, n-heptane, and dimethyl ether (DME) are considered. Spherical symmetry is assumed and thereby the problem is one-dimensional in a spherical coordinate. The hot spot is represented by the following initial temperature distribution:

$$T(r,t=0) = (T_H - T_0)\exp[-(\frac{r}{R})^M] + T_0 \quad (1)$$

where T_H is the central temperature of the hot spot, R characterizes the size of the hot spot and M is a geometric parameter. A Gaussian distribution with M=2 is considered here unless otherwise specified.

For a given value of hot spot size, R, there exists a critical ignition temperature, $T_{H,min}$, such that successful ignition occurs only for $T_H > T_{H,min}$. This critical ignition temperature is obtained and compared by two methods: one is based on the detailed simulation of the transient 1D ignition process while the other is based on the application of the L-W integral. These two methods are introduced below.

2.1 Detailed simulation of the hot spot induced ignition

The transient simulation of hot spot induced ignition process is conducted using the in-house code A-SURF [20-22]. The conservation equations for all species, momentum, and total energy are solved using the finite volume method. Detailed chemistry and transport are considered and CHEMKIN packages [23] are utilized to calculate the detailed thermal-transport properties and reaction rates. Well-validated chemical mechanisms adopted from the literature are used for hydrogen [24], methane [25], n-heptane [26] and DME [27], respectively. The mixture-averaged model is used to evaluate the mass diffusivities for different species. A-SURF has been successfully used in simulations of ignition [28, 29], flame propagation [30, 31], and detonation development [32-34]. Details of governing equations and numerical schemes used in A-SURF are presented in Refs. [20-22].

The computational domain radius is R_W=50 cm. Zero flow speed and zero gradients of mass fractions and temperature are enforced at both boundaries, r=0 and r=R_W. An initially static homogeneous fuel/air mixture with specified equivalence ratio, ϕ, and the initial temperature distribution given by Eq. (1) is considered. Adaptive mesh refinement with the smallest mesh size of 32 μm is used, where grid convergence is achieved to ensure numerical accuracy.

A typical temperature profile history during hot spot induced methane/air ignition is shown in Fig. 1. It is seen that for successful ignition with T_H =1820 K > $T_{H,min}$, heat conduction results in an initial temperature drop around the hot spot. Subsequently, the local temperature increases abruptly due to strong exothermic reactions and the flame kernel can successfully propagate outwardly in a self-sustained manner. For T_H =1810 K < $T_{H,min}$ as shown in Fig. 1(b), the temperature within the hot

spot always decreases since the chemical heat release rate is lower than the rate at which heat is conducted away from the hot spot. Consequently, ignition fails for T_H =1810 K.

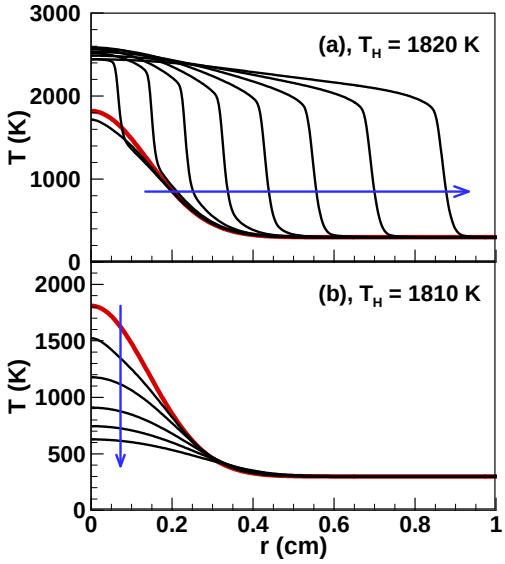

Fig. 1. Evolution of temperature distribution for (a) successful ignition with T_H =1820 K and (b) ignition failure with T_H =1810 K in a stoichiometric CH_4/air mixture with R=2 mm and M=2. The red lines represent initial temperature distributions.

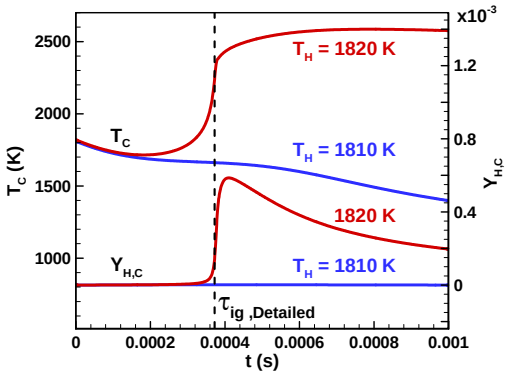

Fig. 2. Change of the central temperature and H mass fraction with time for two cases considered in Fig. 1.

Figure 2 plots the evolution of central temperature and H mass fraction during the hot spot induced ignition process. For T_H =1820 K, an abrupt increment is observed for both temperature and H mass fraction. Therefore, an ignition delay time, $\tau_{ig,\ Detailed}$, can be determined for the hot spot induced ignition (see the vertical dashed line in Fig. 2). For T_H<$T_{H,min}$, the central temperature decreases monotonically and the H radical pool cannot be built up, indicating ignition failure.

Therefore, whether successful ignition is achieved or not can be determined by the evolution of central temperature, T_C. Then the critical ignition temperature, $T_{H,min}$, can be obtained by the method of trial-and-error from detailed simulation with error within ±5 K.

2.2 Prediction method using the Livengood-Wu integral

In the preceding section, the critical ignition temperature is obtained through transient simulation considering detailed chemistry and transport. To reduce the computational cost, an alternative method using the L-W integral is proposed here to predict the critical ignition temperature. The L-W integral is defined as [3]:

$$I = \int_0^t \frac{dt}{\tau_{ig}(t)} \tag{2}$$

where τ_{ig} is the ignition delay at specific conditions.

For hot spot induced ignition, the central temperature is the highest before strong exothermic reactions occur. Therefore, in the L-W integral, Eq. (2), τ_{ig} is the ignition delay at the center (i.e. r=0) of the hot spot whose temperature is T_C. As shown in Fig. 2, the central temperature, T_C, changes with time. During the induction period, the chemical heat release is nearly negligible and so is the convection and pressure increment induced by thermal expansion. Consequently, the evolution of the central temperature, $T_C(t)=T(r=0, t)$, can be approximately obtained by solving the following 1D unsteady heat conduction equation:

$$\frac{\partial T}{\partial t} = \frac{1}{r^2}\frac{\partial}{\partial r}\left(r^2 \alpha \frac{\partial T}{\partial r}\right) \tag{3}$$

where α is the thermal diffusivity of the mixture, depending on temperature and local fuel/air mixture composition. The initial condition is given by Eq. (1) and the boundary conditions are

$$\mathrm{r} = 0: \ \frac{\partial T}{\partial r} = 0; \quad \mathrm{r} = \infty: \ T = T_0 \tag{4}$$

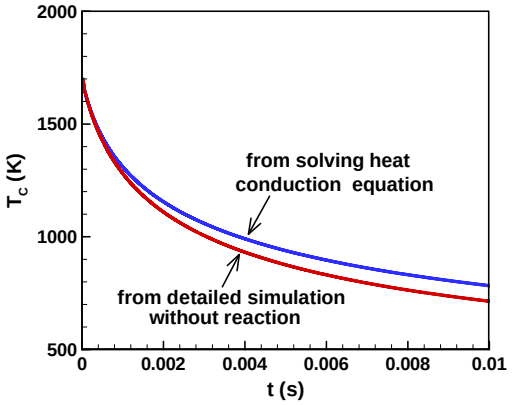

Fig. 3. Change of the central temperature with time in a stoichiometric CH_4/air mixture with T_H=1700 K, R= 2 mm and M=2.

Figure 3 shows the central temperature T_C obtained from the numerical solution of Eq. (3). The results from detailed simulation using A-SURF for non-reactive flow are shown together for comparison. It is observed that T_C from detailed simulation decreases more rapidly. This is primarily due to the extra heat loss caused by convection, which is neglected in Eq. (3). The difference is shown to increase with time. When T_C decreases to 800 K, the maximum difference is 100 K. It is noted that ignition delay increases greatly when the temperature decreases, and that the main contribution to the L-W integral in Eq. (2) is the ignition delay at relatively high temperature (above 1000 K). Therefore, the over-prediction of the central temperature by Eq. (3) has little effect on the value of the L-W integral, as can be seen subsequently in Fig. 6.

After the central temperature is obtained from solving Eq. (3), the corresponding ignition delay, $\tau_{ig}(t)=\tau_{ig}(T_C(t))$, can be obtained from 0D simulation of the constant-pressure homogenous ignition process considering detailed chemistry. Then the L-W integral can be obtained from numerical integration of Eq. (2) with $\tau_{ig}(t)=\tau_{ig}(T_C(t))$. Note that the 0D simulation is decoupled from Eq. (3) since the ignition delay is only a function of temperature.

Figure 4 shows the change of the L-W integral with time during hot spot induced ignition in a stoichiometric CH_4/air mixture. At the beginning with t<0.5 ms, the L-W integral increases rapidly with time. Then the increment becomes smaller due to decreases in the central temperature as shown in Fig. 3. Eventually the L-W integral remains nearly constant for t>1.5 ms. The ignition delay time

for the hot spot induced ignition, $\tau_{ig,H}$, is defined based on the requirement of I=1 and it is represented by the vertical dashed lines in Fig. 4.

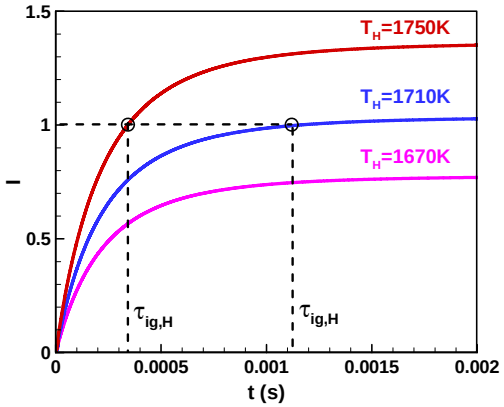

Fig. 4. Change of the L-W integral (based on the central temperature from solving the heat conduction equation) with time for different hot spot temperature in a stoichiometric CH_4/air mixture with R=2 mm and M=2. The symbols denote the hot spot induced ignition delay based on the requirement of I=1.

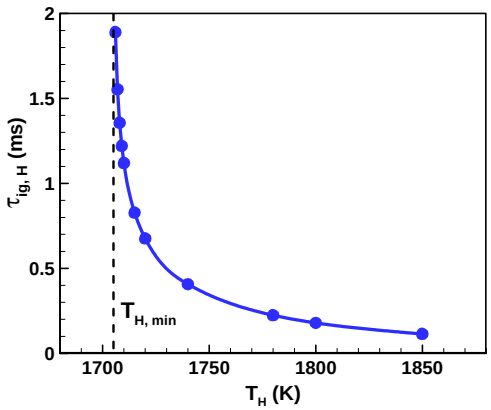

Fig. 5. Change of the ignition delay with hot spot temperature in a stoichiometric CH_4/air mixture with R=2 mm and M=2. The vertical dashed line represents the minimum hot spot temperature for successful ignition.

The ignition delay time for the hot spot induced ignition, $\tau_{ig,H}$, can be calculated for different hot spot temperature, T_H, as shown in Fig. 5. Finally, the critical ignition temperature, $T_{H,min}$, is determined since $\tau_{ig,H}$ approaches infinity for $T_H < T_{H,min}$ (see the vertical dashed line in Fig. 5). As in the current case, $T_{H,min}$ corresponds to a value of 1705 K, which is about 100 K difference from the method identified in Fig. 1 using detailed simulation.

In a brief summary, the L-W approach for the identification of critical ignition temperature from hot spot induced ignition, $T_{H,min}$, includes the following steps: First, the evolution of the temperature at the hot spot center, $T_C=T_C(t)$ is obtained by solving the one-dimensional unsteady heat conduction equation, Eq. (3). Then the L-W integral, Eq. (1) is evaluated based on the homogenous ignition delay time corresponding to the central temperature evolution, $\tau_{ig}(t)=\tau_{ig}(T_C(t))$. The ignition delay time for the hot spot induced ignition, $\tau_{ig,H}$, is determined under the requirement of unity L-W integral (see Fig. 4). Finally, the critical ignition, $T_{H,min}$, is determined by the fact that $\tau_{ig,H}$ becomes infinity for $T_H<T_{H,min}$ (see Fig. 5). The present method based on the L-W integral can reduce the computational cost by two to three orders compared to the detailed transient simulation considering detailed chemistry and transport.

3. Results and discussion

3.1 The critical ignition temperature

The critical ignition temperatures for different fuel/air mixtures and different hot spot features are calculated from the above prediction method using the L-W integral. To assess the performance of the prediction method, the results are compared with those from detailed simulation.

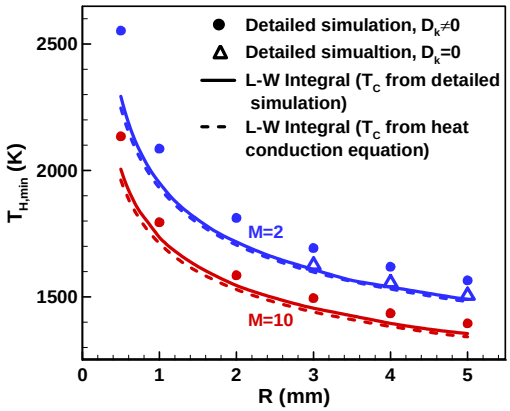

Fig. 6. Change of the critical ignition temperature with hot spot radius for a stoichiometric CH_4/air mixture. D_k is the mass diffusivity of the species and $D_k=0$ ($D_k\neq0$) corresponds to the case that the mass diffusivities of all species are artificially set to zero (unchanged).

Figure 6 shows the change of the critical ignition temperature for hot spot induced ignition, $T_{H,min}$, with the hot spot radius, R, for a stoichiometric CH_4/air mixture. It is observed that $T_{H,min}$ increases substantially with the decrease of the hot spot radius R. This is because the temperature gradient and conductive heat loss are both larger for a smaller hot spot radius. Similarly, for a larger geometric factor of M=10, the hot spot temperature distribution is much flatter than that for M=2, indicating a larger excess energy of the hot spot and smaller conductive heat loss from the center point. Therefore, $T_{H,min}$ for M=10 is always lower than that for M=2.

The critical ignition temperature, $T_{H,min}$, predicted based on the L-W integral is shown to be lower than that from detailed simulation. One possible reason is that in the prediction method using the L-W integral, only heat conduction is considered, while mass diffusion of radicals away from the ignition kernel is neglected. This is the limitation of the present method. At the beginning, there is large temperature gradient in the hot spot, while the radical concentration and its gradient are expected to be small. Therefore, heat conduction dominates over mass diffusion. Nevertheless, the diffusion of radical produced during the induction period (i.e., $t<\tau_{ig,H}$) does prohibit successful ignition. This explains why the critical ignition temperature is under-predicted based on the L-W integral. The under-prediction is expected to increase with the ratio between the time scales for ignition and mass diffusion. This ratio is $B=\tau_{ig,H}/\tau_{Diffusion}$, in which $\tau_{ig,H}$ is the delay time for the forced ignition, and $\tau_{Diffusion}$ is the characteristic diffusion time. We have $\tau_{Diffusion}=R^2/D_R$ (where D_R is the mass diffusivity of the main radical, e.g., H atom) and thereby $B=\tau_{ig,H}D_R/R^2$. With the decrease of hot spot radius R, the ratio B becomes larger and therefore $T_{H,min}$ is more under-predicted by the method based on the L-W integral. This explains the large under-prediction of $T_{H,min}$ for R=0.5 mm as shown in Fig. 6. When the mass diffusivities of all species are artificially set to zero (D_k=0), we have B=0. Consequently, Fig. 6 shows that good agreement is achieved between $T_{H,min}$ predicted based on the L-W integral and that from detailed simulation with D_k=0. Note that when mass diffusion is not included in detailed simulation, successful ignition cannot be achieved for R<3 mm. Besides, comparison between the solid and dashed lines in Fig. 6 indicates that over-prediction (see Fig. 3) of

the central temperature, T_C, by the unsteady heat conduction equation has little influence on the critical ignition temperature, $T_{H,min}$.

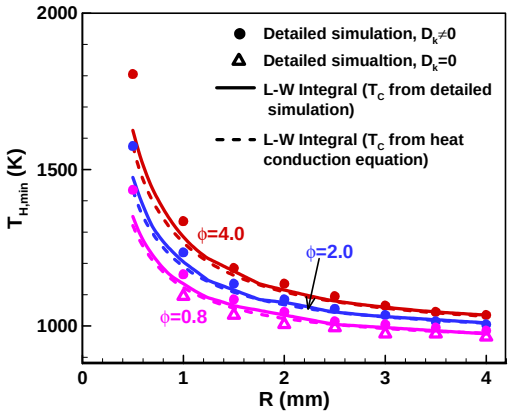

Fig. 7. Change of the critical ignition temperature with hot spot radius for H_2/air mixtures with different equivalence ratios.

Figure 7 shows the results for H_2/air mixtures. The critical ignition temperature from the prediction method is shown to agree well with those from detailed simulations for $R \geq 1$ mm. Compared with CH_4/air mixtures, H_2/air mixtures has much shorter forced ignition time, $\tau_{ig,H}$, due to the higher reactivity of hydrogen. Consequently, compared to CH_4/air, H_2/air has lower ratio between time scales for ignition and mass diffusion, $B=\tau_{ig,H}D_R/R^2$, and thereby more accurate $T_{H,min}$, from the prediction method based on L-W integral. Figure 7 also shows that higher $T_{H,min}$ is required for richer H_2/air mixtures. That is because for H_2/air mixtures, the thermal conductivity and thereby the conductive heat loss from the hot spot increases with the equivalence ratio. Moreover, the reactivity of the fuel- rich H_2/air mixture is also lower, which implies longer duration of heat conduction process before ignition, rendering ignition more difficult.

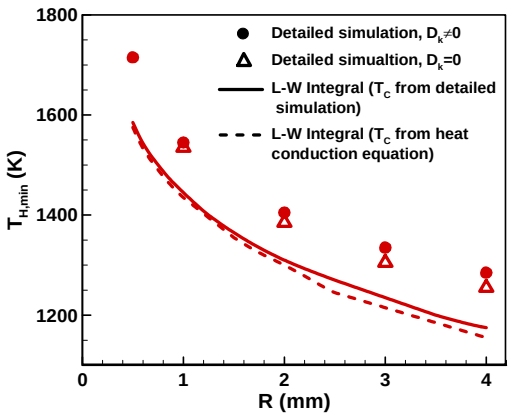

Fig. 8. Change of the critical ignition temperature with hot spot radius for a stoichiometric nC_7H_{16}/air mixture.

Figure 8 shows the critical ignition temperature for nC_7H_{16}/air mixtures. Again, the critical ignition temperature, $T_{H,min}$, predicted based on the L-W integral is shown to be about 100 K lower than that from detailed simulation. Even when the mass diffusivities are artificially set to zero (D_k=0) in the detailed simulation, difference is still observed between the two methods. Similar observations are also obtained for DME/air mixtures. The cause for such difference is not clear and deserves further study. Nevertheless, the relative difference between $T_{H,min}$ from prediction based on the L-W integral and that from detailed simulation is within 10%.

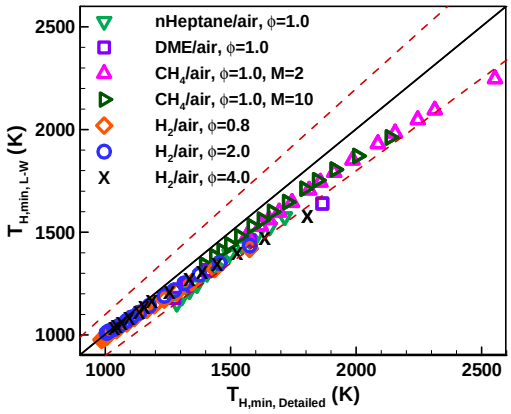

Fig. 9. Comparison of critical ignition temperature from prediction based on the L-W integral, $T_{H,min,\text{L-W}}$, with those from detailed simulations, $T_{H,min,\text{Detailed}}$. The dashed lines denote the border of 10% deviation of $T_{H,min,\text{L-W}}$ from $T_{H,min,\text{Detailed}}$.

Figure 9 compares all the critical ignition temperature from prediction based on the L-W integral ($T_{H,min,\text{L-W}}$) and those from detailed simulations ($T_{H,min,\text{Detailed}}$). Generally, good agreement is shown for critical ignition temperature below 2000 K. The difference becomes larger for higher critical ignition temperature, which corresponds to smaller hot spot radius with larger effects of mass diffusion. Besides, the large stretch rate also affects the propagation of the expanding ignition kernel, especially for mixtures with Lewis number apparently larger than unity [18]. Nevertheless, the method based on the L-W integral can give a conservative prediction of the critical ignition temperature, which is important for safety considerations.

3.2 Effects of low temperature chemistry

For large hydrocarbons such as n-heptane and DME, the low temperature chemistry (LTC) plays an important role for homogeneous autoignition at certain temperature range [35]. However, it is not clear whether the LTC affects the hot spot induced ignition. This is investigated in the following for DME/air mixtures.

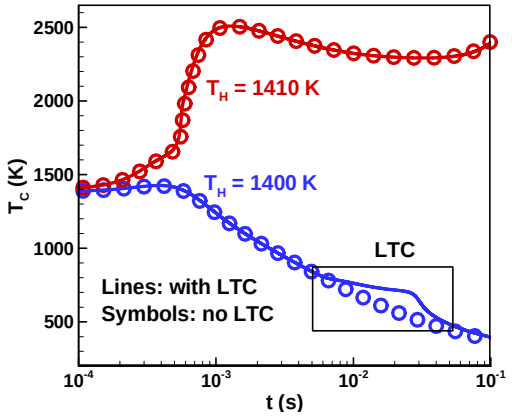

Fig. 10. Effect of LTC on the evolution of central temperature predicted by detailed simulation for a stoichiometric DME/air mixture with R=2 mm and M=2.

We first consider detailed simulations with and without LTC for DME/air mixture. Figure 10 shows that for successful ignition with T_H=1410 K, the evolution of the central temperature, T_C, is not affected by LTC. For unsuccessful ignition with T_H=1400 K, the LTC does affect the central temperature for t>5 ms and T_C<800 K. However, at such low central temperature, the released heat due to LTC is not sufficient enough to balance the conductive heat loss and to prevent ignite failure. Therefore, the LTC is expected to have little effect on the critical ignition temperature.

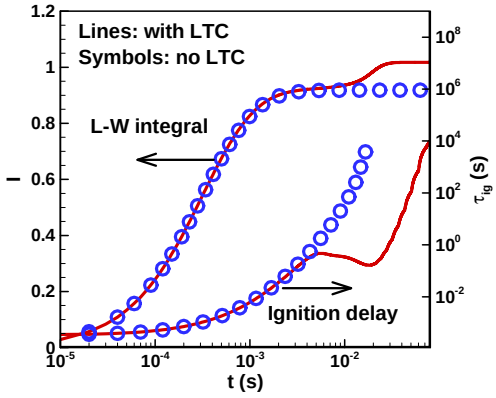

Fig. 11. Effect of LTC on the L-W integral and ignition delay time at the corresponding central temperature from solving the heat conduction equation for a stoichiometric DME/air mixture with T_H=1320 K, R=2 mm and M=2.

The effect of LTC on the L-W integral is shown in Fig. 11. Note that the central temperature of the hot spot changes with time, $T_C=T_C(t)$. Therefore, the corresponding homogeneous ignition delay is a function of time, $\tau_{ig}=\tau_{ig}(T_C(t))$, which is also plotted in Fig. 11. It is seen that the ignition delay time becomes larger when the LTC is not included. The L-W integral becomes slightly larger when the LTC is included. Therefore, the critical ignition temperature, $T_{H,min}$, from the method using the L-W integral should become slightly lower when the LTC is considered.

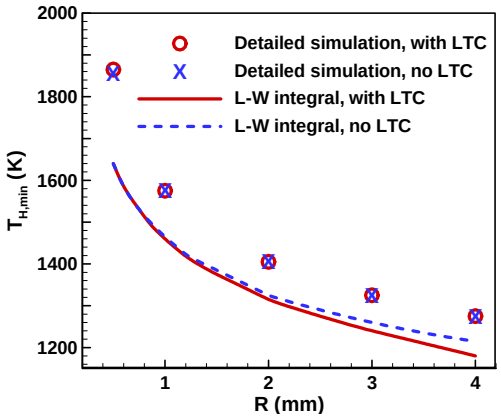

Fig. 12. Effect of low temperature chemistry (LTC) on the critical ignition temperature for a stoichiometric DME/air mixture.

Figure 12 plots the critical ignition temperature from prediction based on the L-W integral and those from detailed simulations with and without LTC. As expected, the LTC effects are almost negligible, indicating that the hot spot induced ignition is mainly controlled by high temperature chemistry (HTC). It is worth noting that the cases considered here are all under the atmospheric pressure. In the internal combustion engines where the pressure is extremely high, the time scale of LTC can become very small. At such conditions, cool flame may occur during the ignition process and the effect of the LTC cannot be neglected [36, 37].

4. Conclusions

A method using the L-W integral is proposed to predict the critical ignition temperature of spot induced ignition in a flammable mixture. In this method, the only partial differential equation needing to be solved is the 1D unsteady heat conduction equation; and the detailed chemistry is only considered in the calculation of 0D homogeneous ignition delay. The computational cost is reduced by two to three orders compared to the detailed transient simulation considering detailed chemistry and transport. This method is used for different fuels including methane, hydrogen, n-heptane, and dimethyl ether. The critical ignition temperature predicted by this method is compared with that from detailed simulation. Good agreement is shown for critical ignition temperature below 2000 K. The difference becomes larger for smaller hot spot radius with shorter mass diffusion time. Nevertheless, the method based on the L-W integral can give a conservative prediction of the critical ignition temperature, which is important for safety considerations. Moreover, it is demonstrated that the hot spot induced ignition is mainly controlled by the HTC and the LTC has little influence.

It is noted that the present study only considers a simplified model with a hot spot fixed inside a quiescent mixture. In practice there might be relative flow between the hot spot and the flammable mixture. Consequently, the ignition process might be affected by convective heat and mass transfer, which merits future study. Besides, even for ignition in a quiescent mixture, the initial ignition kernel is high curved and stretched. The critical ignition condition might be affected by the coupling between stretch and preferential diffusion of heat over the deficient species (i.e., the Lewis number) [18]. Such coupling is not considered in the present method, which is another shortage of this work.

Acknowledgements

This work was supported by National Natural Science Foundation of China (Nos. 91741126 and 51861135309).

References

[1] B. Lewis, G.V. Elbe, Combustion flames and explosive of gases, Academic Press, New York, 1961.

[2] J.B. Heywood, Internal combustion engine fundamentals, McGraw-Hill, New York, 1988.

[3] J.C. Livengood, P.C. Wu, Correlation of autoignition phenomena in internal combustion engines and rapid compression machines, Proc. Combust. Inst. 5 (1955) 347-356.

[4] A. Yates, A. Bell, A. Swarts, Insights relating to the autoignition characteristics of alcohol fuels, Fuel 89 (2010) 83-93.

[5] J.J. Hernandez, M. Lapuerta, J. Sanzargent, Autoignition prediction capability of the Livengood–Wu correlation applied to fuels of commercial interest, Int. J. Eng. Res. 15 (2014) 817-829.

[6] J. Pan, P. Zhao, C.K. Law, H. Wei, A Predictive Livengood-Wu Correlation for Two-stage Ignition, Int. J. Eng. Res. 17 (2016).

[7] M. Tao, D. Han, P. Zhao, An alternative approach to accommodate detailed ignition chemistry in combustion simulation, Combust. Flame 176 (2017) 400-408.

[8] D. Bradley, R.A. Head, Engine autoignition : The relationship between octane numbers and autoignition delay times, Combust. Flame 147 (2006) 171-184.

[9] K.K. Sadabadi, M. Shahbakhti, A.N. Bharath, R.D. Reitz, Modeling of combustion phasing of a reactivity-controlled compression ignition engine for control applications, Int. J. Eng. Res. 17 (2016) 421-435.

[10] M. Reyes, F.V. Tinaut, C. Andrés, A. Pérez, A method to determine ignition delay times for Diesel surrogate fuels from combustion in a constant volume bomb: Inverse Livengood–Wu method, Fuel 102 (2012) 289-298.

[11] A. Miyoshi, Kinetics of autoignition: a simple intuitive interpretation and its relation to the Livengood–Wu integral, Phys. Chem. Chem. Phys. 20 (2018) 10762-10769.

[12] M. Tao, A. Laich, P. Lynch, P. Zhao, On the Interpretation and Correlation of High-Temperature Ignition Delays in Reactors with Varying Thermodynamic Conditions, Int. J. Chem. Kinet. 50 (2018)

410-424.

[13] J.A. Campbell, Appraisal of the hazards of friction-spark ignition of aircraft crash fires, Official Journal of the South African Academy of Family Practice/primary Care 46 (1957) 44-44.

[14] J.L. Urban, *Spot Ignition of Natural Fuels by Hot Metal Particles*, Phd thesis, University of California, Berkeley, 2017.

[15] J.P. Prestemon, T.J. Hawbaker, M. Bowden, J. Carpenter, M.T. Brooks, K.L. Abt, R. Sutphen, S. Scranton, Wildfire Ignitions: A Review of the Science and Recommendations for Empirical Modeling, Technical Report, US Forest Service, Ashevill, NC, 2013.

[16] S.A. Coronel, J. Melguizo-Gavilanes, R. Mével, J.E. Shepherd, Experimental and numerical study on moving hot particle ignition, Combust. Flame 192 (2018) 495-506.

[17] N.N. Semenov, Some Problems in Chemical Kinetics and Reactivity, Princeton University Press, 1958.

[18] Z. Chen, M.P. Burke, Y. Ju, On the critical flame radius and minimum ignition energy for spherical flame initiation, Proc. Combust. Inst. 33 (2011) 1219-1226.

[19] W.K. Liang, C.K. Law, Z. Chen, Ignition of hydrogen/air mixtures by a heated kernel: Role of Soret diffusion, Combust. Flame 197 (2018) 416-422.

[20] Z. Chen, M.P. Burke, Y. Ju, Effects of Lewis number and ignition energy on the determination of laminar flame speed using propagating spherical flames, Proc. Combust. Inst. 32 (2009) 1253-1260.

[21] Z. Chen, Effects of radiation and compression on propagating spherical flames of methane/air mixtures near the lean flammability limit, Combust. Flame 157 (2010) 2267-2276.

[22] P. Dai, Z. Chen, Supersonic reaction front propagation initiated by a hot spot in n-heptane/air mixture with multistage ignition, Combust. Flame 162 (2015) 4183-4193.

[23] R.J. Kee, F.M. Rupley, J.A. Miller, CHEMKIN-II: a Fortran package for the analysis of gas-phase chemical kinetics, Sandia National Laboratory Report SAND89-8009B, 1989.

[24] J. Li, Z. Zhao, A. Kazakov, F.L. Dryer, An updated comprehensive kinetic model of hydrogen

combustion, Int. J. Chem. Kinet. 36 (2010) 566–575.

[25] G. Smith, D.M. Golden, M. Frenklach, N.W. Moriarty, B. Eiteneer, M. Goldenberg, C.T. Bowman, R.K. Hanson, S. Song, W.C. Gardiner, Jr., V.V. Lissianski, Z. Qin, The GRI-Mech 3.0 chemical kinetic mechanism, http://www.me.berkeley.edu/gri_mech/.

[26] S. Liu, J.C. Hewson, J.H. Chen, H. Pitsch, Effects of strain rate on high-pressure nonpremixed n-heptane autoignition in counterflow, Combust. Flame 137 (2004) 320-339.

[27] Z. Zhao, M. Chaos, A. Kazakov, F.L. Dryer, Thermal decomposition reaction and a comprehensive kinetic model of dimethyl ether, Int. J. Chem. Kinet. 40 (2008) 1-18.

[28] Y. Wang, W. Han, Z. Chen, Effects of fuel stratification on ignition kernel development and minimum ignition energy of n-decane/air mixtures, Proc. Combust. Inst. 37 (2019) 1623-1630.

[29] Z.S. Li, X.L. Gou, Z. Chen, Effects of hydrogen addition on non-premixed ignition of iso-octane by hot air in a diffusion layer, Combust. Flame 199 (2019) 292-300.

[30] Z. Chen, Effects of radiation absorption on spherical flame propagation and radiation-induced uncertainty in laminar flame speed measurement, Proc. Combust. Inst. 37 (2017) 1129-1136.

[31] M. Faghih, H.Y. Li, X.L. Gou, Z. Chen, On laminar premixed flame propagating into autoigniting mixtures under engine-relevant conditions, Proc. Combust. Inst. 37 (2019) 4673-4680.

[32] P. Dai, C.K. Qi, Z. Chen, Effects of initial temperature on autoignition and detonation development in dimethyl ether/air mixtures with temperature gradient, Proc. Combust. Inst. 36 (2017) 3643-3650.

[33] P. Dai, Z. Chen, S. Chen, Y. Ju, Numerical experiments on reaction front propagation in n-heptane/air mixture with temperature gradient, Proc. Combust. Inst. 35 (2015) 3045-3052.

[34] C. Qi, Z. Chen, Effects of temperature perturbation on direct detonation initiation, Proc. Combust. Inst. 36 (2017) 2743-2751.

[35] F. Battin-Leclerc, Detailed chemical kinetic models for the low-temperature combustion of hydrocarbons with application to gasoline and diesel fuel surrogates, Prog. Energy Combust. Sci. 34 (2008) 440-498.

[36] Y. Ju, C.B. Reuter, O.R. Yehia, T. Farouk, S.H. Won, Dynamics of cool flames, Prog. Energy Combust. Sci. 75 (2019) 100787.

[37] W. Zhang, M. Faqih, X. Gou, Z. Chen, Numerical study on the transient evolution of a premixed cool flame, Combust. Flame 187 (2018) 129-136.

Figure captions

Fig. 1 Evolution of temperature distribution for (a) successful ignition with T_H =1820 K and (b) ignition failure with T_H =1810 K in a stoichiometric CH_4/air mixture with R=2 mm and M=2. The red lines represent initial temperature distributions.

Fig. 2 Change of the central temperature and H mass fraction with time for two cases considered in Fig. 1.

Fig. 3 Change of the central temperature with time in a stoichiometric CH_4/air mixture with T_H=1700 K, R= 2 mm and M=2.

Fig. 4 Change of the L-W integral (based on the central temperature from solving the heat conduction equation) with time for different hot spot temperature in a stoichiometric CH_4/air mixture with R=2 mm and M=2. The symbols denote the hot spot induced ignition delay based on the requirement of I=1.

Fig. 5 Change of the ignition delay with hot spot temperature in a stoichiometric CH_4/air mixture with R=2 mm and M=2. The vertical dashed line represents the minimum hot spot temperature for successful ignition.

Fig. 6 Change of the critical ignition temperature with hot spot radius for a stoichiometric CH_4/air mixture. D_k is the mass diffusivity of the species and D_k=0 (D_k≠0) corresponds to the case that the mass diffusivities of all species are artificially set to zero (unchanged).

Fig. 7 Change of the critical ignition temperature with hot spot radius for H_2/air mixtures with different equivalence ratios.

Fig. 8 Change of the critical ignition temperature with hot spot radius for a stoichiometric nC_7H_{16}/air mixture.

Fig. 9 Comparison of critical ignition temperature from prediction based on the L-W integral, $T_{H,min,L\text{-}W}$, with those from detailed simulations, $T_{H,min,Detailed}$. The dashed lines denote the border of 10% deviation of $T_{H,min,L\text{-}W}$ from $T_{H,min,Detailed}$.

Fig. 10 Effect of LTC on the evolution of central temperature predicted by detailed simulation for a stoichiometric DME/air mixture with R=2 mm and M=2.

Fig. 11 Effect of LTC on the L-W integral and ignition delay time at the corresponding central temperature from solving the heat conduction equation for a stoichiometric DME/air mixture with T_H=1320 K, R=2mm and M=2.

Fig. 12 Effect of low temperature chemistry (LTC) on the critical ignition temperature for a stoichiometric DME/air mixture.